T-domains is accompanied by the formation of crystallographic domains as a result of spontaneous magnetostriction. But mostly this is very small. Each of the T-domains may split into 180° domains.

The magnetization process in ferromagnets possessing T-domains is similar to the previously described magnetization of an easy-axis ferromagnet in a magnetic field directed at an oblique angle. First the displacement process allows those 180° domains that are directed unfavourably in each T-domain to disappear, and then the rotation process follows.

In easy-plane antiferromagnets, the T-domain structure is destroyed by a small magnetic field and the antiferromagnetic vector **L** in the whole specimen becomes directed perpendicular to the applied magnetic field, as was explained in Section 1.5.3.

There are four kinds of T-domains in cubic antiferromagnets, in which the vectors **L** are directed parallel or perpendicular to the four ⟨111⟩ axes. Such a T-domain structure can be destroyed only when the applied magnetic field is so strong that the antiferromagnetic order is destroyed at a spin-flip transition.

1.5.4.3. *Ferroic domains*

Aizu (1970) gave a classification of domain formation when a crystal undergoes a transition from an unordered to a magnetically ordered state that has a lower point-group symmetry (see also Section 3.1.1). The unordered state (called the prototype phase) has a grey point group. The number of elements in this group is equal to the product of the number of elements in the point group of the ordered state (called the ferroic state) times the number of domains. Aizu found that there are 773 possible combinations of the point-group symmetries of the prototype and the ferroic state, if crystallographically inequivalent orientations of the subgroup in the group of the prototype are distinguished. These 773 combinations are called ferroic species and are characterized by a symbol giving first the point group of the prototype, then the letter F, then the point group of the ferroic state and finally a letter between parentheses if different orientations are possible. As an example, the $2'$ axis of the ferroic state is parallel to the fourfold axis of the prototype in $4221'\mathrm{F}2'(p)$ and perpendicular to it in $4221'\mathrm{F}2'(s)$.

Let us discuss the ferroic states of rhombohedral transition-metal oxides given in Table 1.5.3.4. The paramagnetic prototype has point group $\bar{3}m1'$. The four monoclinic ferroic species have six domains ('orientation states') each, which form three pairs of 180° domains ('time-conjugate orientation states'). All four species are 'fully ferroelastic', *i.e.* the three pairs show different orientations of the spontaneous strain; two of the four species ($\bar{3}m1'\mathrm{F}2'/m'$ and $\bar{3}m1'\mathrm{F}2/m$) are also 'fully ferromagnetic' because all six domains have different orientations of the spontaneous magnetization. Switching a domain into another with a different orientation of the spontaneous strain can be achieved by applying mechanical stress. If the domain was spontaneously magnetized, the orientation of the magnetization is changed simultaneously. Similarly, a domain can be switched into another with a different orientation of the spontaneous magnetization by means of a magnetic field. If the two spontaneous magnetizations have different directions (not just opposite sign), the direction of the spontaneous strain will change at the same time.

The Aizu classification is of interest for technological applications because it gives an overall view not only of domain formation but also of the possibilities for domain switching.

1.5.5. Weakly non-collinear magnetic structures

As was indicated above (see Tables 1.5.3.3 and 1.5.3.6), certain magnetic space groups allow the coexistence of two different types of magnetic ordering. Some magnetic structures can be described as a superposition of two antiferromagnetic structures with perpendicular antiferromagnetic vectors $\mathbf{L}_\alpha$. Such structures may be called weakly non-collinear antiferromagnets. There can also be a superposition of an antiferromagnetic structure **L** with a ferromagnetic one **M** (with $\mathbf{L} \perp \mathbf{M}$). This phenomenon is called weak ferromagnetism. We shall demonstrate in this section why one of the magnetic vectors has a much smaller value than the other in such mixed structures.

1.5.5.1. *Weak ferromagnetism*

The theory of weak ferromagnetism was developed by Dzyaloshinskii (1957*a*). He showed that the expansion of the thermodynamic potential $\tilde{\Phi}$ may contain terms of the following type: $L_i M_k$ $(i, k = x, y)$. Such terms are invariant with respect to the transformations of many crystallographic space groups (see Section 1.5.3.3). If there is an antiferromagnetic ordering in the material ($L_i \neq 0$) and the thermodynamic potential of the material contains such a term, the minimum of the potential will be obtained only if $M_k \neq 0$ as well. The term $L_i M_k$ is a relativistic one. Therefore this effect must be small.

We shall consider as an example the origin of weak ferromagnetism in the two-sublattice antiferromagnets $MnCO_3$, $CoCO_3$ and $NiCO_3$, discussed in Section 1.5.3.1. The following analysis can be applied also to the four-sublattice antiferromagnet α-Fe_2O_3 (assuming $\mathbf{L}_1 = \mathbf{L}_2 = 0$, $\mathbf{L}_3 = \mathbf{L}$). All these rhombohedral crystals belong to the crystallographic space group $\boldsymbol{D}_{3d}^6 = R\bar{3}c$. The thermodynamic potential $\tilde{\Phi}$ for these crystals was derived in Section 1.5.3.3. For the case of a two-sublattice antiferromagnet, one has to add to the expression (1.5.3.26) the invariant (1.5.3.24):

$$\tilde{\Phi} = (A/2)\mathbf{L}^2 + (B/2)\mathbf{M}^2 + (a/2)L_z^2 + (b/2)M_z^2 + d(L_x M_y - L_y M_x) - \mathbf{MH}. \quad (1.5.5.1)$$

The coefficients of the isotropic terms (A and B) are of exchange origin. They are much larger than the coefficients of the relativistic terms (a, b, d). Minimization of $\tilde{\Phi}$ for a fixed value of $\mathbf{L}^2$ and $\mathbf{H} = 0$ gives two solutions:

(1) $\mathbf{L} \parallel Oz$ $(L_x = L_y = 0,\ \mathbf{M} = 0)$. $FeCO_3$ and the low-temperature modification of α-Fe_2O_3 possess such purely antiferromagnetic structures.

(2) $\mathbf{L} \perp Oz$ $[M_x = (d/B)L_y,\ M_y = (d/B)L_x,\ M_z = 0]$. This structure exhibits a spontaneous ferromagnetic moment

$$M_D = (M_x^2 + M_y^2)^{1/2} = (d/B)L. \quad (1.5.5.2)$$

The magnetic moment M_D is smaller than the magnetization of the sublattices ($M_0 = L/2$) in the ratio $2d/B$. This phenomenon is therefore called weak ferromagnetism. The vectors $\mathbf{M}_D$ and **L** are mutually perpendicular. Their direction in the plane is determined by the sixth-order terms of the anisotropy energy (see Section 1.5.3.2). This anisotropy is extremely small in most materials. The vectors of magnetization of the sublattices $\mathbf{M}_0$ are deflected by a small angle $\varphi \simeq 2d/B$ away from the direction of the antiferromagnetic axis **L** in such weak ferromagnets (see Fig. 1.5.5.1).

Weak ferromagnetism was first observed in the following trigonal crystals: the high-temperature modification of haematite, α-Fe_2O_3 (Townsend Smith, 1916; Néel & Pauthenet, 1952), $MnCO_3$ (Borovik-Romanov & Orlova, 1956) and later also in $CoCO_3$, $NiCO_3$ and $FeBO_3$. In accordance with theory, weak ferromagnetism does not occur in trigonal crystals with a positive anisotropy coefficient a. Such crystals become easy-axis antiferromagnets. Of this type are $FeCO_3$ and the low-temperature modification of α-Fe_2O_3. For four-sublattice antiferromagnets, the sequence of the directions of the magnetic moments of the sublattices is also essential. For example, the structures of the types $\boldsymbol{A}_1$ and $\boldsymbol{A}_2$ (see Fig. 1.5.3.4 and Table 1.5.3.3) do not exhibit weak ferromagnetism.

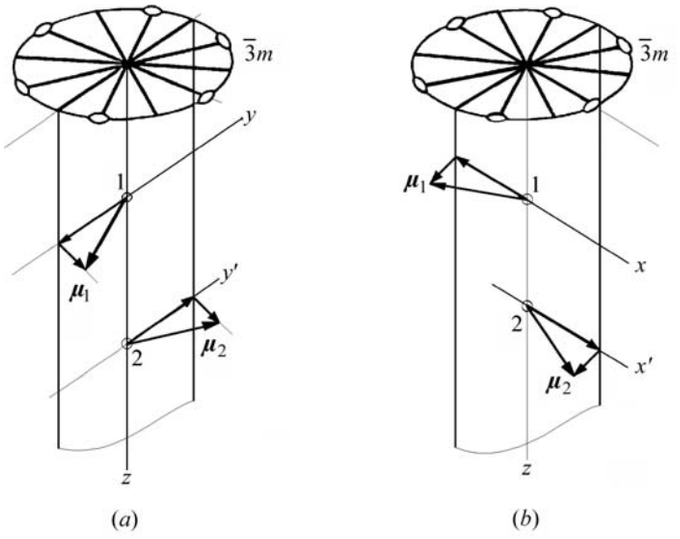

Fig. 1.5.5.1. Diagrams demonstrating two weakly ferromagnetic structures in rhombohedral crystals with two magnetic ions in the primitive cell (compare with Fig. 1.5.3.1). (*a*) Magnetic space group $P2/c$; (*b*) magnetic space group $P2'/c'$.

The behaviour of weak ferromagnets in magnetic fields applied perpendicular ($H_\perp$) and parallel ($H_\parallel$) to the trigonal axis is described by the following relations:

$$M_\perp = M_D + \chi_\perp H_\perp, \quad M_\parallel = \chi_\parallel H_\parallel, \tag{1.5.5.3}$$

where

$$\chi_\perp = 1/B, \quad \chi_\parallel = 1/(B+b). \tag{1.5.5.4}$$

An external magnetic field can freely rotate the ferromagnetic moment in the basal plane of the easy-plane weak ferromagnets under consideration because their anisotropy in the basal plane is extremely small. During such a rotation, both vectors **M** and **L** move simultaneously as a rigid structure. On the other hand, it is impossible to deflect the vector $\mathbf{M}_D$ out of the basal plane, as this is forbidden by symmetry. This is illustrated by the magnetization curves plotted in Fig. 1.5.5.2, which confirm the relations (1.5.5.3).

It is worth mentioning that when the weakly ferromagnetic structure is rotated in the basal plane, a change of the magnetic space groups occurs in the following order: $P2/c \leftrightarrow P\bar{1} \leftrightarrow P2'/c' \leftrightarrow P\bar{1} \leftrightarrow P2/c \leftrightarrow \ldots$. Each of these symmetry transformations corresponds to a second-order phase transition. Such transitions are allowed because $P\bar{1}$ is a subgroup of both groups $P2/c$ and $P2'/c'$.

NiF_2 was one of the first weak ferromagnets to be discovered (Matarrese & Stout, 1954). In the paramagnetic state, it is a tetragonal crystal. Its crystallographic space group is $\boldsymbol{D}_{4h}^{14} = P4_2/mnm$. In the ordered state its magnetic point group is $\boldsymbol{D}_{2h}(\boldsymbol{C}_{2h}) = mm'm'$ and the vectors **L** and **M** are directed along two twofold axes (one of which is primed) in the plane perpendicular to the former fourfold axis (see Fig. 1.5.5.3*a*). The invariant term responsible for the weak ferromagnetism in tetragonal fluorides has the form

$$d(L_x M_y + L_y M_x). \tag{1.5.5.5}$$

The anisotropy of the crystals of NiF_2 and the relation given above for the invariant lead to the same dependence on the magnetic field as for trigonal crystals. However, the anisotropy of the magnetic behaviour in the basal plane is much more complicated than for rhombohedral crystals (see Bazhan & Bazan, 1975). The anisotropy constant K_1 is positive for most other fluorides (MnF_2, FeF_2 and CoF_2) and their magnetic structure is described by the magnetic point group

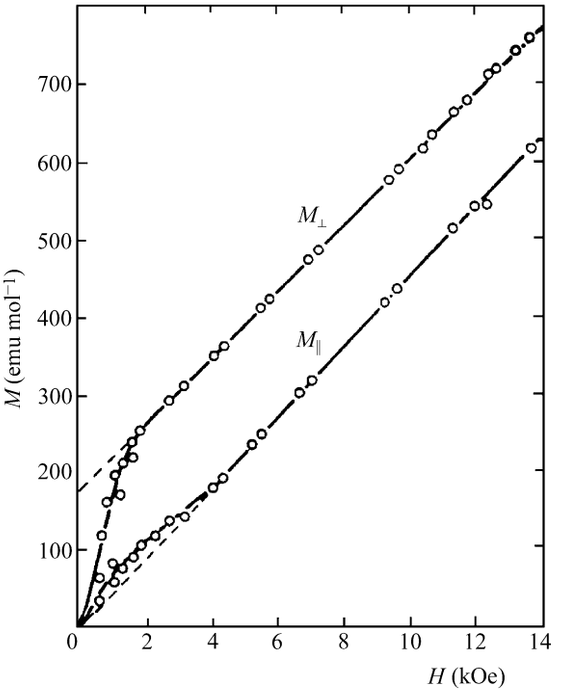

Fig. 1.5.5.2. Dependence of magnetization $M_\perp$ and $M_\parallel$ on the magnetic field H for the weak ferromagnet $MnCO_3$ at 4.2 K (Borovik-Romanov, 1959*a*).

$\boldsymbol{D}_{4h}(\boldsymbol{D}_{2h}) = 4'/mmm'$. They are easy-axis antiferromagnets without weak ferromagnetism.

The interaction described by the invariant $d(L_x M_y - L_y M_x)$ in equation (1.5.5.1) is called Dzyaloshinskii–Moriya interaction. It corresponds to the interaction between the spins of neighbouring ions, which can be represented in the form

$$\mathbf{d}[\mathbf{S}_i \times \mathbf{S}_j], \tag{1.5.5.6}$$

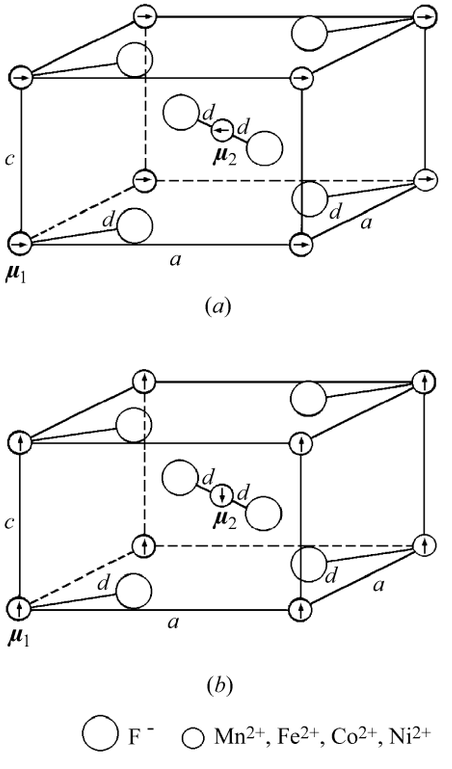

Fig. 1.5.5.3. Magnetic structures of fluorides of transition metals. (*a*) The weak ferromagnet NiF_2; (*b*) the easy-axis antiferromagnets MnF_2, FeF_2 and CoF_2.

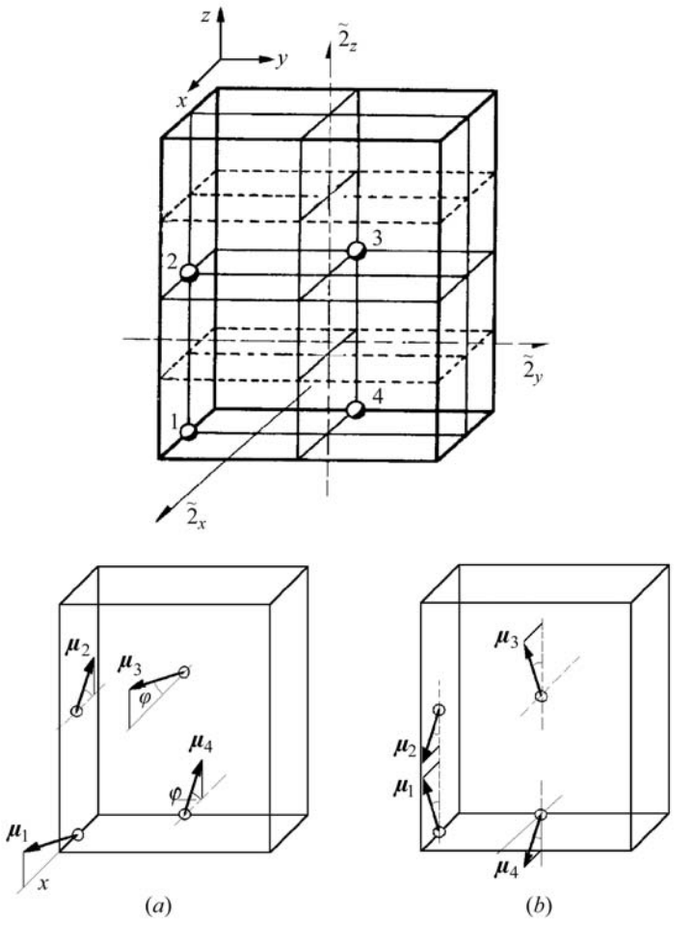

Fig. 1.5.5.4. Magnetic structures of orthoferrites and orthochromites RMO_3. (Only the transition-metal ions are shown; the setting *Pbnm* is used.) (*a*) $\boldsymbol{G}_x\boldsymbol{F}_z$ weakly ferromagnetic state; (*b*) $\boldsymbol{G}_z\boldsymbol{F}_x$ weakly ferromagnetic state.

where the vector **d** has the components $(0, 0, d_z)$. Terms of such type are allowed by symmetry for crystals that in the paramagnetic state belong to certain space groups of the trigonal, tetragonal and hexagonal systems. In some groups of the tetragonal system, weak ferromagnetism is governed by the term $d(L_xM_y + L_yM_x)$ (as for NiF_2) and in the orthorhombic system by $(d_1L_iM_k + d_2L_kM_i)$, $(i, k = x, y, z)$. In the monoclinic system, the latter sum contains four terms. The weak ferromagnetism in most groups of the hexagonal and cubic systems is governed by invariants of fourth and sixth order of L_i, M_k. Turov (1963) determined for all crystallographic space groups the form of the invariants of lowest order that allow for collinear or weakly non-collinear antiferromagnetic structures a phase transition into a state with weak ferromagnetism. The corresponding list of the numbers of the space groups that allow the transition into an antiferromagnetic state with weak ferromagnetism is given in Table 1.5.5.1. The form of the invariant responsible for weak ferromagnetism is also displayed in the table. Turov (1963) showed that weak ferromagnetism is forbidden for the triclinic system, for the six trigonal groups with point groups $C_3 = 3$ or $C_{3i} = \bar{3}$, and the 12 cubic groups with point groups $T = 23$ or $T_h = m\bar{3}$.

The microscopic theory of the origin of weak ferromagnetism was given by Moriya (1960*a*,*b*, 1963). In this chapter, however, we have restricted our consideration to the phenomenological approach to this problem.

A large number of orthorhombic orthoferrites and orthochromites with the formula RMO_3 (where R is a trivalent rare-earth ion and M is Fe^{3+} or Cr^{3+}) have been investigated in many laboratories (*cf.* Wijn, 1994). Some of them exhibit weak ferromagnetism. The space group of these compounds is $\boldsymbol{D}_{2h}^{16} = Pnma$ in the paramagnetic state. The primitive cell is the same in the paramagnetic and magnetically ordered states. It contains four magnetic transition-metal ions (see Fig. 1.5.5.4). They determine to a large extent the properties of orthoferrites (outside the region of very low temperatures). For a four-sublattice antiferromagnet, there are four possible linear combinations of the sublattice vectors, which define three types of antiferromagnetic vectors $\mathbf{L}_\alpha$ and one ferromagnetic vector **F** [see relations (1.5.3.2) and Table 1.5.3.1]. The exchange interaction in these compounds governs magnetic structures, which to a first approximation are described by the following antiferromagnetic vector (which is usually denoted by the symbol $\boldsymbol{G}$):

$$\boldsymbol{G} = \mathbf{L}_2 = (N/4)(\boldsymbol{\mu}_1 - \boldsymbol{\mu}_2 + \boldsymbol{\mu}_3 - \boldsymbol{\mu}_4). \qquad (1.5.5.7)$$

In the case of orthoferrites, the other two antiferromagnetic vectors $\mathbf{L}_1$ and $\mathbf{L}_3$ [see relations (1.5.3.2)] are named $\boldsymbol{A}$ and $\boldsymbol{C}$, respectively.

The magnetic structure of the compounds under consideration is usually called the $\boldsymbol{G}_i$ or $\boldsymbol{G}_i\boldsymbol{F}_k$ state. Depending on the signs and

Table 1.5.5.1. *The numbers of the crystallographic space groups that allow a phase transition into a weakly ferromagnetic state and the invariants of lowest order that are responsible for weak ferromagnetism*

Note that the standard numbering of space groups is used in this table, not the one employed by Turov (1963).

System	Nos. of the space groups	Invariants	Case No.
Monoclinic	3–15	M_xL_y, M_zL_y, M_yL_x, M_yL_z	1
Orthorhombic	16–74	M_xL_y, M_yL_x	2
		M_yL_z, M_zL_y	3
		M_xL_z, M_zL_x	4
Tetragonal	75–88	$M_xL_y + M_yL_x$, $M_xL_x - M_yL_y$	5
	89–142	$M_xL_y - M_yL_x$	6
		$M_xL_y + M_yL_x$	7
		$M_xL_x - M_yL_y$	8
Trigonal	149–167	$M_xL_y - M_yL_x$	9, 10
Hexagonal	168–176	$M_z(L_x \pm iL_y)^3$, $(M_x \pm iM_y)(L_x \pm iL_y)^2L_z$	11
	177–194	$M_xL_y - M_yL_x$	12
		$iM_z[(L_x + iL_y)^3 - (L_x - iL_y)^3]$, $i[(M_x + iM_y)(L_x + iL_y)^2 - (M_x - iM_y)(L_x - iL_y)^2]L_z$	13
		$M_z[(L_x + iL_y)^3 + (L_x - iL_y)^3]$, $[(M_x + iM_y)(L_x + iL_y)^2 + (M_x - iM_y)(L_x - iL_y)^2]L_z$	14
Cubic	207–230	$M_xL_x(L_y^2 - L_z^2) + M_yL_y(L_z^2 - L_x^2) + M_zL_z(L_x^2 - L_y^2)$	15

the values of the anisotropy constants, there are three possible magnetic states:

$$\text{(I)} \quad \boldsymbol{G}_x\boldsymbol{F}_z \quad L_{2x} \neq 0; \quad M_{Dz} \neq 0, \tag{1.5.5.8}$$

$$\text{(II)} \quad \boldsymbol{G}_y \quad L_{2y} \neq 0; \quad \mathbf{M}_D = 0, \tag{1.5.5.9}$$

$$\text{(III)} \quad \boldsymbol{G}_z\boldsymbol{F}_x \quad L_{2z} \neq 0; \quad M_{Dx} \neq 0. \tag{1.5.5.10}$$

The magnetic structures (I) and (III) are weak ferromagnets. They are displayed schematically in Fig. 1.5.5.4. Both are described by the same magnetic point group $\boldsymbol{D}_{2h}(\boldsymbol{C}_{2h})$ yet in different orientations: $m'm'm$ (*i.e.* $2'_x/m'_x\ 2'_y/m'_y\ 2_z/m_z$) for structure (I) and $mm'm'$ (*i.e.* $2_x/m_x\ 2'_y/m'_y\ 2'_z/m'_z$) for structure (III). The magnetic point group of structure (II) is $\boldsymbol{D}_{2h} = mmm$.

Weak ferromagnetism is observed in boracites with chemical formula $M_3B_7O_{13}X$ (where M = Co, Ni and X = Br, Cl, I). These compounds are unique, being simultaneously antiferromagnets, weak ferromagnets and ferroelectrics. Section 1.5.8.3 is devoted to these ferromagnetoelectrics.

Concerning the magnetic groups that allow weak ferromagnetism, it should be noted that, as for any ferromagnetism, weak ferromagnetism is allowed only in those space groups that have a trivial magnetic Bravais lattice. There must be at least two magnetic ions in the primitive cell to get antiferromagnetic order. Among the 31 magnetic point groups that admit ferromagnetism (see Table 1.5.2.4), weak ferromagnetism is forbidden in the magnetic groups belonging to the tetragonal, trigonal and hexagonal systems. Twelve magnetic point groups that allow weak ferromagnetism remain. These groups are listed in Table 1.5.5.2.

A material that becomes a weak ferromagnet below the Néel temperature T_N differs from a collinear antiferromagnet in its behaviour above T_N. A magnetic field applied to such a material above T_N gives rise to an ordered antiferromagnetic state with vector **L** directed perpendicular and magnetization **M** parallel to the field. Thus, as in usual ferromagnets, the magnetic symmetry of a weak ferromagnet in a magnetic field is the same above and below T_N. As a result, the magnetic susceptibility has a maximum at $T = T_N$ [like the relations (1.5.3.34) and (1.5.3.35)]. This is true only if the magnetic field is aligned along the easy axis for weak ferromagnetism. Fig. 1.5.5.5 shows the anomalous anisotropy of the temperature dependence of the magnetic susceptibility in the neighbourhood of T_N for weak ferromagnets.

Similar anomalies in the neighbourhood of T_N are observed in materials with a symmetry allowing a transition into a weakly ferromagnetic state for which the sign of the anisotropy constant causes their transition into purely antiferromagnetic states.

1.5.5.2. *Other weakly non-collinear magnetic structures*

A thermodynamic potential $\tilde{\Phi}$ of the form (1.5.5.1) may give rise not only to the weak ferromagnetism considered above but also to the reverse phenomenon. If the coefficient B (instead of A) changes its sign and $b > 0$, the material will undergo a transition into a slightly canted ferromagnetic structure, in which $M_s \gg L_D$ and the expression for L_D is

Table 1.5.5.2. *Magnetic point groups that allow weak ferromagnetism*

Schoenflies	Hermann–Mauguin
$\boldsymbol{C}_1$	1
$\boldsymbol{C}_i$	$\bar{1}$
$\boldsymbol{C}_2$	2
$\boldsymbol{C}_2(\boldsymbol{C}_1)$	$2'$
$\boldsymbol{C}_s$	m
$\boldsymbol{C}_s(\boldsymbol{C}_1)$	m'
$\boldsymbol{C}_{2h}$	$2/m$
$\boldsymbol{C}_{2h}(\boldsymbol{C}_i)$	$2'/m'$
$\boldsymbol{D}_2(\boldsymbol{C}_2)$	$22'2'$
$\boldsymbol{C}_{2v}(\boldsymbol{C}_2)$	$m'm'2$
$\boldsymbol{C}_{2v}(\boldsymbol{C}_s)$	$m'm2'$
$\boldsymbol{D}_{2h}(\boldsymbol{C}_{2h})$	$mm'm'$

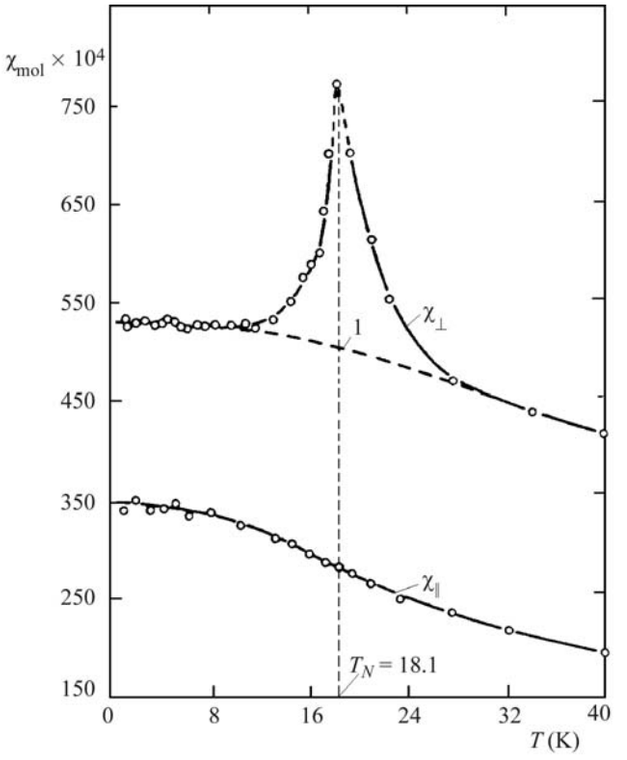

Fig. 1.5.5.5. Temperature dependence of the susceptibility for $CoCO_3$ (Borovik-Romanov & Ozhogin, 1960).

$$L_D = (d/B)M_{s\perp}. \tag{1.5.5.11}$$

Experimental detection of such structures is a difficult problem and to date no-one has observed such a phenomenon.

The thermodynamic potential $\tilde{\Phi}$ of a four-sublattice antiferromagnet may contain the mixed invariant [see (1.5.3.24)]

$$d_1(L_{1x}L_{2y} - L_{1y}L_{2x}). \tag{1.5.5.12}$$

Such a term gives rise to a structure in which all four vectors of sublattice magnetization $\mathbf{M}_\alpha$ form a star, as shown in Fig. 1.5.5.6 (see also Fig. 1.5.1.3*b*). The angle 2α between the vectors $\boldsymbol{\mu}_1$ and $\boldsymbol{\mu}_3$ (or $\boldsymbol{\mu}_2$ and $\boldsymbol{\mu}_4$) is equal to d_1/A_2 if the main antiferromagnetic structure is defined by the vector $\mathbf{l}_2$ [see relation (1.5.3.2)]. Such a structure may occur in Cr_2O_3. In most orthoferrites discussed above, such non-collinear structures are observed for all three cases: purely antiferromagnetic ($\boldsymbol{G}_y$) and weakly ferromagnetic ($\boldsymbol{G}_x\boldsymbol{F}_z$ and $\boldsymbol{G}_z\boldsymbol{F}_x$). The structure $\boldsymbol{G}_y$ is not coplanar. Apart from the main antiferromagnetic vector **G** aligned along the y axis, it possesses two other antiferromagnetic vectors: **A** (aligned along the x axis) and **C** (aligned along the z axis). The weakly ferromagnetic structure $\boldsymbol{G}_x\boldsymbol{F}_z$ has an admixture of the $\boldsymbol{A}_y$ antiferromagnetic structure.

The helical (or spiral) structure described in Section 1.5.1.2.3 and depicted in Fig. 1.5.1.4 is also a weakly non-collinear antiferromagnetic structure. As mentioned above, this structure consists of atomic layers in which all the magnetic moments are

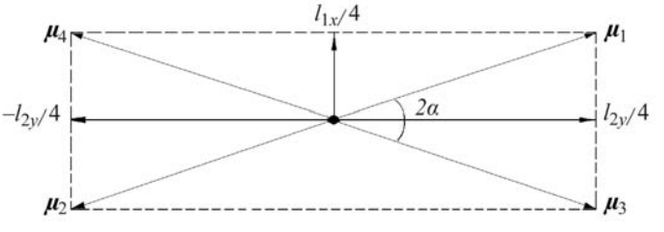

Fig. 1.5.5.6. A weakly non-collinear magnetic structure corresponding to (1.5.5.12).

parallel to each other and parallel to the layer. The magnetizations of neighbouring layers are antiparallel to a first approximation; but, more specifically, there is a small deviation from a strictly antiparallel alignment. The layers are perpendicular to a vector **k**, which is parallel to the axis of the helix. The two mutually perpendicular antiferromagnetic vectors $\mathbf{L}_\alpha$ are both perpendicular to **k**. These vectors define the helical structure by the following relation for the density of the magnetization $\mathbf{M}(\mathbf{r})$ in the layer with the coordinate **r** (Dzyaloshinskii, 1964; Andreev & Marchenko, 1980):

$$\mathbf{M}(\mathbf{r}) = \mathbf{L}_1 \sin \mathbf{kr} - \mathbf{L}_2 \cos \mathbf{kr}. \qquad (1.5.5.13)$$

Most helical structures are incommensurate, which means that the representation defined by the vector **k** does not satisfy the Lifshitz condition (see Section 1.5.3.3).

1.5.6. Reorientation transitions

In many materials, the anisotropy constants change sign at some temperature below the critical temperature. As a result, the direction of the vector **L** (or $\mathbf{M}_s$) changes relative to the crystallographic axes. Correspondingly, the magnetic symmetry of the material also changes. Such phase transitions are called reorientation transitions.

Cobalt is a typical ferromagnet and experiences two such reorientation transitions. It is a hexagonal crystal, which at low temperatures behaves as an easy-axis ferromagnet; its magnetic point group is $\boldsymbol{D}_{6h}(\boldsymbol{C}_{6h}) = 6/mm'm'$. If the anisotropy energy were described by the relations (1.5.3.6) and (1.5.3.7) with only one anisotropy constant K_1, the change of the sign of this constant would give rise to a first-order transition from an easy-axis to an easy-plane antiferromagnet. This transition would occur at the temperature T_c at which $K_1(T) = 0$. In fact, the polar angle θ which determines the direction of the spontaneous magnetization increases progressively over a finite temperature interval. The behaviour of θ during the process of this reorientation may be obtained by minimizing the expression of the anisotropy energy (1.5.3.10), which contains two anisotropy coefficients K_1 and K_2. If $K_2 > 0$, the minimum of U_a corresponds to three magnetic phases, which belong to the following magnetic point groups:

(1) $\boldsymbol{D}_{6h}(\boldsymbol{C}_{6h}) = 6/mm'm'$; for this phase $\theta = 0, \pi$. It is realized at temperatures $T < T_1 = 520$ K, where $K_1 > 0$.

(2) $\boldsymbol{C}_{2h}(\boldsymbol{C}_i) = 2'/m'$; for this phase $\sin\theta = \pm(-K_1/2K_2)^{1/2}$. It is realized at temperatures $T_1 = 520 < T < T_2 = 580$ K, where $-2K_2 < K_1 < 0$.

(3) $\boldsymbol{D}_{2h}(\boldsymbol{C}_{2h}) = mm'm'$; for this phase $\theta = \pi/2$. It is realized at temperatures $T_2 = 580 < T < T_c = 690$ K, where $K_1 < -2K_2$.

The low-temperature phase is of the easy-axis type and the high-temperature phase is of the easy-plane type. The intermediate phase is called the angular phase. The two second-order phase transitions occur at temperatures which are the roots of the two equations

$$K_1(T_1) = 0; \quad K_1(T_2) + 2K_2(T_2) = 0. \qquad (1.5.6.1)$$

The chain of these transitions (including the transition to the paramagnetic state at $T = T_c$) may be represented by the following chain of the corresponding magnetic point groups:

$$\begin{aligned} \boldsymbol{D}_{6h}(\boldsymbol{C}_{6h}) = 6/mm'm' &\longleftrightarrow \boldsymbol{C}_{2h}(\boldsymbol{C}_i) = 2'/m' \\ &\longleftrightarrow \boldsymbol{D}_{2h}(\boldsymbol{C}_{2h}) = mm'm' \\ &\longleftrightarrow (\boldsymbol{D}_{6h} + \boldsymbol{R}\boldsymbol{D}_{6h}) = 6/mmm1'. \end{aligned}$$

In Co and most of the other ferromagnets, the rotation of the spontaneous magnetization described above may be obtained by applying an external magnetic field in an appropriate direction. In many antiferromagnets, there occur similar reorientation transitions, which cannot be achieved by means of a magnetic field.

The first reorientation transition in antiferromagnets was observed in haematite (α-Fe_2O_3), which at room temperature is a weak ferromagnet with magnetic structure $\boldsymbol{A}_{3x}$ or $\boldsymbol{A}_{3y}$ (see Tables 1.5.3.3 and 1.5.3.4 in Section 1.5.3.1). Morin (1950) found that the weak ferromagnetism in haematite disappears below $T_M \simeq 260$ K. At low temperature, haematite becomes an easy-axis antiferromagnet with the structure $\boldsymbol{A}_{3z}$. Unlike in cobalt, the transition at T_M is a first-order transition in haematite. This is so because the anisotropy constant K_2 is negative in haematite. As a result, there are only two solutions for the angle θ that lead to a minimum of the anisotropy energy $U_a(3)$ [(1.5.3.9)], $\theta = 0$ if $K_1 > -K_2$ and $\theta = \pi/2$ if $K_1 < -K_2$. The transition temperature T_M is defined by

$$K_1(T_M) + K_2(T_M) = 0. \qquad (1.5.6.2)$$

There is the following change in the magnetic space groups at this transition:

$$R\bar{3}c' \overset{T_M}{\longleftrightarrow} \begin{cases} P2/c & (1.5.6.3) \\ P2'/c' & (1.5.6.4) \end{cases}$$

Which of the two groups is realized at high temperatures depends on the sign of the anisotropy constant $K'_\perp$ in equation (1.5.3.9). Neither of the high-temperature magnetic space groups is a subgroup of the low-temperature group. Therefore the transition under consideration cannot be a second-order transition.

Reorientation transitions have been observed in many orthoferrites and orthochromites. Orthoferrites of Ho, Er, Tm, Nd, Sm and Dy possess the structure $\boldsymbol{G}_x\boldsymbol{F}_z$ [see (1.5.5.8)] at room temperature. The first five of them undergo reorientation transitions to the structure $\boldsymbol{G}_z\boldsymbol{F}_x$ at lower temperatures. This reorientation occurs gradually, as in Co. Both vectors **L** and $\mathbf{M}_D$ rotate simultaneously, as shown in Fig. 1.5.6.1. These vectors remain perpendicular to each other, but the value of $\mathbf{M}_D$ varies from $(d_1/B)L$ for M_{Dz} to $(d_2/B)L$ for M_{Dx}. The coefficients d_1 and d_2 belong to the terms L_xM_z and L_zM_x, respectively. The following magnetic point groups are observed when these transitions occur:

$$\frac{2'_x}{m'_x}\frac{2'_y}{m'_y}\frac{2_z}{m_z} \overset{T_1}{\longleftrightarrow} \frac{2'_y}{m'_y} \overset{T_2}{\longleftrightarrow} \frac{2_x}{m_x}\frac{2'_y}{m'_y}\frac{2'_z}{m'_z}. \qquad (1.5.6.5)$$

Anomalies typical for second-order transitions were observed at the temperatures T_1 and T_2. The interval $T_2 - T_1$ varies from 10 to 100 K.

At low temperatures, $DyFeO_3$ is an easy-axis antiferromagnet without weak ferromagnetism – $\boldsymbol{G}_y$. It belongs to the trivial magnetic point group $\boldsymbol{D}_{2h} = mmm$. At $T_M = 40$ K, $DyFeO_3$ transforms into a weak ferromagnet $\boldsymbol{G}_x\mathbf{F}_z$. This is a first-order reorientation transition of the type

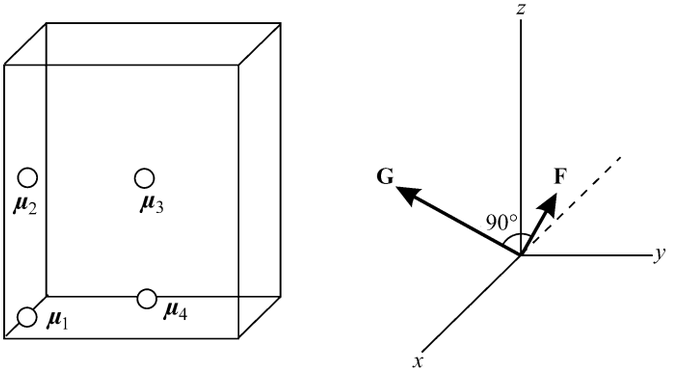

Fig. 1.5.6.1. Schematic representation of the rotation of the vectors **G** and **F** (in the *xz* plane) at a reorientation transition in orthoferrites.